



저작자표시-비영리-변경금지 2.0 대한민국

이용자는 아래의 조건을 따르는 경우에 한하여 자유롭게

- 이 저작물을 복제, 배포, 전송, 전시, 공연 및 방송할 수 있습니다.

다음과 같은 조건을 따라야 합니다:



저작자표시. 귀하는 원저작자를 표시하여야 합니다.



비영리. 귀하는 이 저작물을 영리 목적으로 이용할 수 없습니다.



변경금지. 귀하는 이 저작물을 개작, 변형 또는 가공할 수 없습니다.

- 귀하는, 이 저작물의 재이용이나 배포의 경우, 이 저작물에 적용된 이용허락조건을 명확하게 나타내어야 합니다.
- 저작권자로부터 별도의 허가를 받으면 이러한 조건들은 적용되지 않습니다.

저작권법에 따른 이용자의 권리는 위의 내용에 의하여 영향을 받지 않습니다.

이것은 [이용허락규약\(Legal Code\)](#)을 이해하기 쉽게 요약한 것입니다.

[Disclaimer](#)

공학석사학위논문

부분 예혼합 합성가스 화염에서  $N_2$ ,  $CO_2$   
희석이 배출물 특성에 미치는 영향

Effects of  $N_2$ ,  $CO_2$  Dilution on Emission Characteristics of  
Partially Premixed Syngas Flame

2015년 2월

서울대학교 대학원

기계항공공학부

오 재 요

# 부분 예혼합 합성가스 화염에서 N<sub>2</sub>, CO<sub>2</sub> 희석이 배출물 특성에 미치는 영향

Effects of N<sub>2</sub>, CO<sub>2</sub> Dilution on Emission Characteristics of  
Partially Premixed Syngas Flame

지도교수 윤 영 빈

이 논문을 공학석사 학위논문으로 제출함

2014년 10월

서울대학교 대학원  
기계항공공학부  
오 재 요

오재요의 공학석사 학위논문을 인준함

2014년 12월

위원장

鄭仁碩



부위원장

윤영빈



위원

오재요



## **Abstract**

# **Effects of N<sub>2</sub>, CO<sub>2</sub> Dilution on Emission Characteristics of Partially Premixed Syngas Flame**

Jaeyo Oh

Department of Mechanical and Aerospace Engineering

The Graduate School

Seoul National University

Coal thermal power generation had advantage in plenty reserves and low cost, but it had pollution problem. Integrated coal-gasification combined-cycle power system (IGCC) is improved power generation technology which reduce sulfur oxides, nitrogen oxide, and carbon oxide largely. IGCC has been being developed and constructed globally, also domestically Taean IGCC plant is now being constructed. Gasified fuel called syngas contains H<sub>2</sub>, so to prevent flash-back combustion should be non-premixed. In this study, dilution is investigated to control NO<sub>x</sub> formed in non-premixed combustion.

We conducted combustion test in model gas turbine combustor equipped with copied GE7EA nozzle varying diluent and dilution placement to understand which factor affects emission characteristics in dilution condition. Concentration of

emission was measured in exhaust pipe, cross section of flame was attained by Abel transformed photograph of OH chemiluminescence.

Result of diluent comparison test showed that there was other factor which affected emission characteristics in addition to temperature decrease caused by diluent, through flame structure analysis the factor was identified as degree of mixing determined by fuel-air jet momentum ratio. Comparing dilution placement, fuel-side dilution reduced more NO<sub>x</sub> because proportion of diluent that passed through flame front was bigger in fuel-side dilution than that in air-side dilution. CO was emitted below 10 ppm over almost the whole operation region, but CO emission increased sharply at low equivalence ratio dilution condition in which CO incompletely combusted.

**Keywords: IGCC, Gas turbine, NO<sub>x</sub>, Diluent, Dilution placement, Flame structure, Jet momentum ratio**

**Student Number: 2013-22485**

# Contents

Chapter 1	INTRODUCTION.....	1
1.1	NO <sub>x</sub> emission.....	1
1.2	Jet in crossflow .....	4
1.3	Overview of present work.....	6
Chapter 2	APPARATUS AND EXPERIMENTAL METHOD	
	.....	8
2.1	Apparatus .....	8
2.2	Experimental method.....	12
2.2.1	NO <sub>x</sub> measurement .....	12
2.2.2	Flame image acquisition .....	14
2.3	Test condition.....	16
Chapter 3	RESULTS AND DISCUSSION.....	18
3.1	NO <sub>x</sub> emission characteristics.....	18
3.1.1	Comparison of diluents.....	20

3.1.2	Comparison of dilution placement.....	31
3.2	CO emission characteristics.....	35
Chapter 4	CONCLUSION.....	39
Appendix A.	Correction of Emission Concentration .....	41
Bibliography	.....	44
Abstract in Korean	.....	48

## List of Tables

Table 2.1	Specification of TESTO 350K. ....	12
Table 2.2	Specification of the optical band pass filter. ....	14
Table 2.3	Test condition. ....	16
Table 3.1	Flame structure change depending on dilution ratio (jet momentum ratio), $T_{inlet}=600K$ . ....	27
Table 3.2	Flame intensity change depending on dilution placement and dilution ratio, $T_{inlet}=600K$ .....	34



## List of Figures

Fig. 1.1	Schematic of jet in crossflow .....	5
Fig. 2.1	Schematic of model gas turbine combustor .....	8
Fig. 2.2	Location of the thermocouples.....	9
Fig. 2.3	Front view of the swirler .....	10
Fig. 2.4	Schematic of the flow in the nozzle .....	10
Fig. 2.5	Princeton instrument PI-MAX 2 (16bit ICCD).	14
Fig. 2.6	Schematic of the dilution placements of the combustor.....	17
Fig. 3.1	NO <sub>x</sub> concentrations with respect to inlet air temperature.....	19
Fig. 3.2	NO <sub>x</sub> concentrations with respect to equivalence ratio, $T_{inlet}=600K$ .....	19
Fig. 3.3	NO <sub>x</sub> concentrations with respect to diluent heat capacity, $\phi=0.6$ , $T_{inlet}=600K$ . .....	21
Fig. 3.4	NO <sub>x</sub> concentrations with respect to diluent heat capacity, $\phi=1.0$ , $T_{inlet}=600K$ . .....	21
Fig. 3.5	Flame image of the combustor.....	23

Fig. 3.6	Flame structure change depending on jet momentum ratio, $T_{inlet}=600K$ . ....	24
Fig. 3.7	NOx concentrations with respect to diluent heat capacity, $\phi=1.0$ , $T_{inlet}=600K$ . ....	26
Fig. 3.8	Jet momentum ratio with respect to diluent heat capacity, $\phi=1.0$ .....	26
Fig. 3.9	Flame structure map, $T_{inlet}=600K$ .....	29
Fig. 3.10	NOx concentrations with respect to diluent heat capacity, $\phi=0.6$ , $T_{inlet}=600K$ . ....	30
Fig. 3.11	NOx concentrations with respect to diluent heat capacity, $\phi=1.0$ , $T_{inlet}=600K$ . ....	30
Fig. 3.12	NOx concentrations with respect to dilution placement, $\phi=0.5$ , $T_{inlet}=600K$ . ....	32
Fig. 3.13	NOx concentrations with respect to dilution placement, $\phi=1.0$ , $T_{inlet}=600K$ . ....	32
Fig. 3.14	CO concentrations with respect to inlet air temperature.....	36
Fig. 3.15	CO concentrations with respect to equivalence ratio, $T_{inlet}=600K$ . ....	36

Fig. 3.16	CO concentrations with respect to diluent, $T_{inlet}=600K$ .....	37
Fig. 3.17	CO concentrations with respect to dilution placement, $T_{inlet}=600K$ . ....	38

# Chapter 1 INTRODUCTION

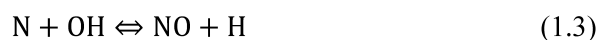
## 1.1 NO<sub>x</sub> emission

Nitrogen oxide is one of air contaminants. It is compound of nitrogen and oxygen. There are some kind of nitrogen oxide, for example nitric oxide (NO), dinitrogen trioxide (N<sub>2</sub>O<sub>3</sub>), dinitrogen pentoxide (N<sub>2</sub>O<sub>5</sub>). Among them, nitric oxide (NO) and nitrogen dioxide (NO<sub>2</sub>) is formed during combustion and they are referred to as NO<sub>x</sub>. In atmosphere NO<sub>x</sub> is harmful to human, it reacts with water to form acid rain, and it is one source of photochemical smog. Therefore NO<sub>x</sub> emission must be restricted.

During combustion, NO<sub>x</sub> is formed by four mechanism – thermal or Zeldovich mechanism, the Fenimore or prompt mechanism, the N<sub>2</sub>O intermediate mechanism, and the NNH mechanism [1]. In these mechanism nitrogen that takes part in reaction comes from not fuel but air.

### 1) Thermal mechanism

Three steps of Zeldovich mechanism are shown below. First two steps are Zeldovich's and by adding third reaction it is referred to as extended Zeldovich mechanism.



Temperature affects this mechanism largely. First step of the mechanism need large activation energy (319,050 kJ/kmol), so this mechanism is important at high temperature above 1800 K.

## 2) Prompt mechanism

Prompt mechanism is related to combustion of hydrocarbons. During combustion of hydrocarbons, NO<sub>x</sub> is formed early before it is produced by thermal mechanism. This NO<sub>x</sub> formation is caused by reaction between hydrocarbon radical and nitrogen.



These products form NO consequently.

## 3) N<sub>2</sub>O intermediate mechanism

This mechanism is operated mainly in low equivalence ratio ( $\phi < 0.8$ ) and low temperature. Therefore, it is considered importantly lean premixed combustion in gas turbine combustor.



#### 4) NNH mechanism

NNH mechanism consists of two steps.



This mechanism is important in oxidation process of hydrogen and hydrocarbons which have high proportion of hydrogen.

## 1.2 Jet in crossflow

Jet in crossflow is that a flow which jets from an orifice intersects with the fluid which is running over the orifice and two flows interact with each other. It can be applied in many area such as fuel injector, dilution in gas turbine combustor, V/STOL aircraft, cooling of gas turbine blade. The main parameter which determines the characteristics of the flow is jet to crossflow momentum ratio or momentum flux ratio [2]. Jet to crossflow momentum flux ratio,  $r$ , is

$$r = \left( \frac{\rho_j U_j^2}{\rho_{cf} U_{cf}^2} \right)^{1/2} \quad (1.11)$$

Here  $\rho$  is density,  $U$  is velocity, and subscripts  $j$  and  $cf$  present jet and crossflow respectively. In the case of intersection between same density flow,

$$r = \frac{U_j}{U_{cf}} \quad (1.12)$$

Various properties of the flow are changed depending on the momentum ratio. Among them, penetration of jet into surrounding flow and mixing between jet and the flow grow as the ratio increases. A schematic of this phenomenon is shown in figure 1.1.

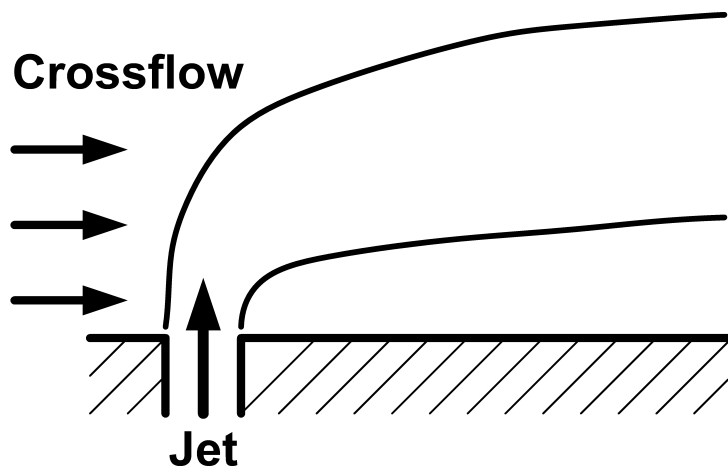
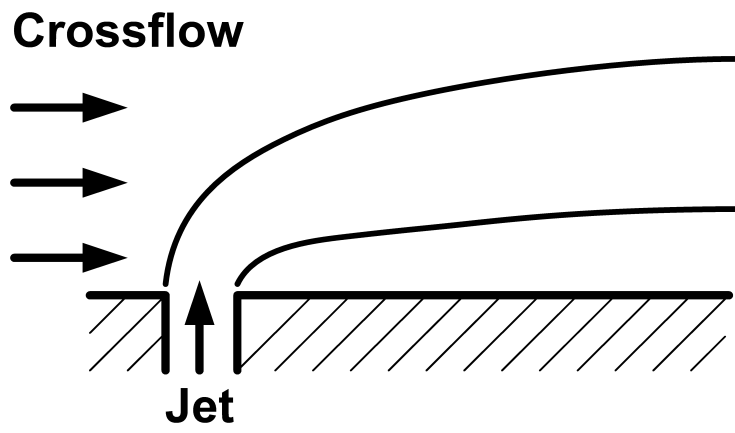


Figure 1.1 Schematic of jet in crossflow (a) at low jet momentum ratio, (b) at high momentum ratio.



### 1.3 Overview of present works

Coal thermal power generation has been being used to supply energy for a long time. Coal has advantage in plenty reserves and low cost, But this power generation also has problem as well. When coal is burned directly many contaminants are emitted, and among these sulfur oxide, nitrogen oxide, and carbon dioxide are representative pollutants. Integrated coal gasification combined cycle (IGCC) is developed to solve this pollution problem. By gasification, carbon capture and storage process, coal becomes syngas and significant amounts of sulfur oxide, nitrogen oxide, and carbon dioxide are removed before combustion. Pre-combustion process as this also reduces cost for decreasing emission of pollutants. Syngas produced by gasification consists of  $H_2$  and  $CO$ . because  $H_2$  has high flame speed, combustor must be non-premixed to prevent flashback. But in non-premixed combustion flame temperature is higher than that in premixed combustion, to control formation of  $NO_x$  dilution is applied.

Liu and Sanderson conducted combustion test in actual Siemens gas turbine combustor. The combustor was premixed type, they varied Wobbe Index (WI) by dilution and the diluents were  $N_2$  and  $CO_2$ .  $NO_x$  emission characteristics was investigated, momentum ratio of fuel jet to air was mentioned as one factor because it seemed affects pre-mixedness between fuel and air. Comparison of diluents shown that more  $NO_x$  was produced with  $N_2$  dilution [3].

Fackler et al. investigated dilution effect of  $N_2$ ,  $CO_2$  conducting experimental and numerical studies. As a result of comparison between  $N_2$  and  $CO_2$  as diluent, it was confirmed that  $N_2$  dilution produced more  $NO_x$  than  $CO_2$  dilution. Chemical reactor

network model was used to understand the effects of  $N_2$  and  $CO_2$  to reaction [4].

Lee et al. studied  $NO_x$  emission characteristics in partially-premixed model gas turbine combustor comparing  $N_2$ ,  $CO_2$ , and steam as diluent.  $NO_x$  reduction caused by dilution was different according to diluent because diluent heat capacity was different respectively. From this result, it was shown that  $NO_x$  reduction graph expressed as function of diluent heat capacity was almost same for three diluents [5].

Weiland and Strakey conducted combustion test in lean direct injection (LDI) combustor using hydrogen as fuel. Effect of dilution placement – fuel-side dilution and air-side dilution – was investigated in several respects. For  $NO_x$  emission characteristics, it was shown that dilution placement affected peak flame temperature, consequently  $NO_x$  was influenced by dilution placement and the degree varied depending on equivalence ratio [6].

In this study emission characteristics of partially premixed  $H_2/CO$  syngas in dilution and factors which affect the characteristics were investigated. Diluent was divided into  $N_2$  and  $CO_2$ , dilution placement into fuel-side and air-side. To confirm which factor affected  $NO_x$  emission, flame structure was analyzed and the flame image was gained by photograph of OH chemiluminescence and Abel transform. In dilution placement comparison, it was confirmed that dilution effect varied depending on the dilution placement due to peak flame temperature and it was based on the result of Weiland and Strakey. From these results, we suggested that these results could be applied in nozzle design and in determination of combustor operation range.

# Chapter 2 APPARATUS AND EXPERIMENTAL METHOD

## 2.1 Apparatus

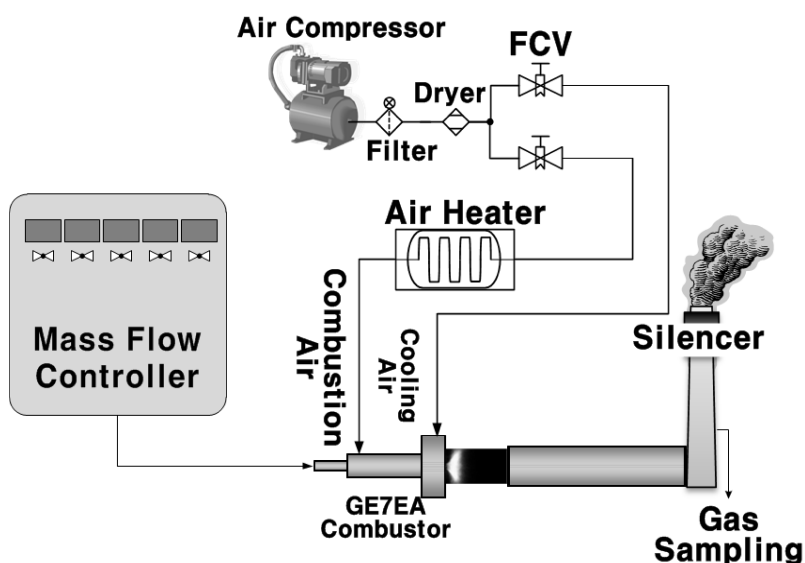


Figure 2.1 Schematic of model gas turbine combustor.

Figure 2.1 shows a schematic of overall experimental apparatus. The main components are air compressor, air heater, mass flow controller, and model gas turbine combustor. The air compressor supplies compressed air to combustor. The mass flow controller controls mass flow rate of provided fuels and air. The compressed air passes through the air heater and is heated to test condition. The model gas turbine combustor consists of a swirl injector, quartz tube which enable optical access, and exhaust duct in which exhaust emissions are measured. And to

have a general idea of temperature tendency during combustion in combustor, seven thermocouples were equipped. One of the thermocouples that is located closely after flame is R-type that can measure up to about 2000 K, and the others are K-type that is durable up to about 1300 K. Exact flame temperature could not be measured, but tendency of temperature change depending on dilution and equivalence ratio could be understood. Figure 2.2 shows the location of the temperature measurement point briefly.

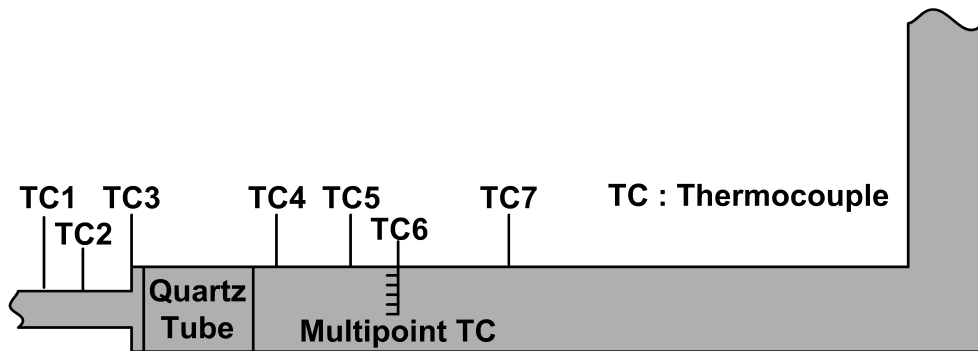


Figure 2.2 Location of the thermocouples.

In order to investigate the characteristics of the non-premixed  $H_2/CO$  syngas flame, 1/3 scaled-down model of GE7EA partially premixed nozzle was used. We studied for one can combustor of whole burner. The nozzle is the axial-flow type swirl injector which has 14 swirl vane and  $45^\circ$  swirl angle. In addition to number of swirl vane and degree of swirl angle swirl number is also important parameter of swirl injector because it represents swirl intensity. Swirl number  $S_n$  is determined by the geometry of the injector and calculated by following equation.

$$S_n = \frac{2}{3} \left[ \frac{1 - \left( \frac{D_{swirl-in}}{D_{swirl-out}} \right)^3}{1 - \left( \frac{D_{swirl-in}}{D_{swirl-out}} \right)^2} \right] \tan \varphi \quad (2.1)$$

$D_{swirl-in}$ ,  $D_{swirl-out}$ , and  $\varphi$  are inner and outer diameter of swirler, and swirl angle. The swirl number of this swirl injector calculated by the equation is 0.83 [7]. The front view of the swirler is shown in figure 2.3.

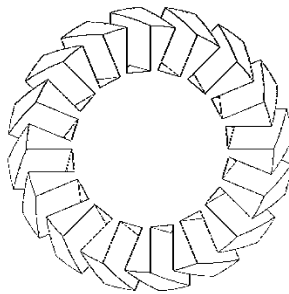


Figure 2.3 Front view of the swirler.

The swirl is main stream, it is air-stream. The fuel is injected to air stream being crossed like jet-in-crossflow to enhance mixing of the supplied air and fuel before combustion. Figure 2.4 shows the schematic of the flow.

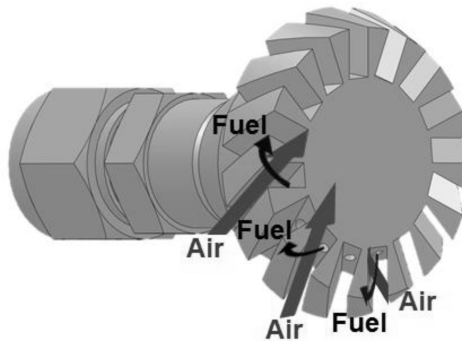


Figure 2.4 Schematic of the flow in the nozzle.

This nozzle is partially-premixed type and mixing length is about 2.7 mm. Mixing length is the distance between fuel hole and dump plane. In the nozzle the geometry that affects the degree of mixing is fixed, but mixedness can be changed by the characteristics of the jet-in-crossflow.

## 2.2 Experimental method

### 2.2.1 Emission measurement

In order to understand the emission characteristics of H<sub>2</sub>/CO syngas flame, we measured concentration of exhaust gas as NO<sub>x</sub>, CO, and O<sub>2</sub> etc. in the exhaust duct. The measurement was conducted using TESTO 350K. The specification is presented in table 2.1.

Resolution	NO <sub>x</sub>	0.1 ppm
	CO	1 ppm
Sampling rate	1 Hz	

Table 2.1 Specification of TESTO 350K

The emissions were measured for 5 seconds after they reached stable state. The value of NO<sub>x</sub> concentration were almost same at the stable state, but CO emission did not reach the very stable state. The exhaust O<sub>2</sub> concentration was measured to correct emission concentration. The emission concentration unit is ppm (v), parts per million (volume), it depends on the mass of emission and total volume of exhaust gas. So, in order to compare emission of a gas turbine with emission of other equipment or other conditions in same device measured emission concentration must be corrected by a standard. The standard is 15% O<sub>2</sub> in exhaust gas for gas turbine, while 3% O<sub>2</sub> for boiler. According to definition, measured emission concentration is corrected by following equation [1].

$$C_{i, \text{ corrected to 15\% O}_2} = C_{i, \text{ measured}} \left( \frac{N_{\text{total, raw}}}{N_{\text{total, corrected to 15\% O}_2}} \right) \quad (2.2)$$

$C_i$  is concentration of component  $i$ ,  $N_{\text{total}}$  is number of total moles in product gas.

Generally, without dilution, the formula is expressed as

$$C_{i, @ 15\% \text{ O}_2} [ppm] = C_{i, \text{ measured}} [ppm] \cdot \left( \frac{20.9-15}{20.9-C_{\text{O}_2, \text{ measured}} [\%]} \right) \quad (2.3)$$

But if this equation is used in dilution condition, some error will occur because measured concentration of  $i$  and  $\text{O}_2$  will become small due to augmented total mole number of exhaust gas. So, using equation (2.3) at dilution condition, emission concentration seems to be smaller than actual value. Therefore other formula which corrects measured concentration of emission exactly is needed. The correction equation which refers to Elkady [8] is shown in equation (2.4).

$$C_{i @ 15\% \text{ O}_2} [ppm] = C_{i, \text{ measured}} [ppm] \cdot \left[ 0.02278 \cdot \frac{(\alpha+2.381)}{(\alpha-C_{\text{O}_2, \text{ measured}})} \right] \quad (2.4)$$

$\alpha$  is mole fraction of  $\text{O}_2$  in oxidizer containing diluent. This formula is matched to the  $\text{H}_2/\text{CO}$  syngas fuel composition. The derivation is presented in appendix A.



## 2.2.2 Flame image acquisition

Flame image was captured by a high-speed ICCD camera through quartz tube. In order to visualize the flame we took a photograph of OH chemiluminescence emitted during combustion because OH radical indicates reaction region. The emitted radiation has particular wave length, so to measure the chemiluminescence the camera was equipped with an optical band pass filter. The high-speed ICCD camera is shown in figure 2.5 and the specification of the optical band pass filter is presented in table 2.2.



Figure 2.5 Princeton instrument PI-MAX 2 (16bit ICCD)

Optical filter	Center of wavelength	Band-pass wavelength
OH*	307.1 nm	15 nm

Table 2.2 Specification of the optical band pass filter

The captured chemiluminescence image is overlapped image of a 3D flame. In order to obtain a cross section of the central axis, abel transform was used [9]. The

gained flame image shows the flame structure and represents the flame temperature, reaction rate, and heat release rate.

## 2.3 Test condition

Item	Value	Unit
H <sub>2</sub> :CO	29:71 (Tae'an)	vol %
Air flow rate	0.015	Kg/s
Inlet air temperature	300, 400, 500, 600	K
Equivalence ratio	0.4 ~ 1.0	
Diluent	N <sub>2</sub> , CO <sub>2</sub>	
Dilution placement	Fuel-side, Air-side	
Dilution ratio	0 ~ 200	%

Table 2.3 Test condition

Table 2.3 shows overall test condition. In this test, fuel composition copied that of Tae'an IGCC plant. For investigating the emission characteristics of H<sub>2</sub>/CO syngas flame, inlet air temperature and equivalence ratio was changed. The air flow rate was constant, the fuel flow rate was changed to determine the equivalence ratio.

For understanding the factor which affects the emission characteristics of H<sub>2</sub>/CO syngas flame diluent, dilution placement were chosen as main variable. As diluent, N<sub>2</sub> and CO<sub>2</sub> were used for some reasons. First, N<sub>2</sub> and CO<sub>2</sub> have different properties as molecular weight, specific heat. And they have actual applications in industrial field. N<sub>2</sub> is used in IGCC mainly because N<sub>2</sub> is produced in air separation process that supplies O<sub>2</sub> to gasifier and it can be used in gas turbine combustor. CO<sub>2</sub> is also used in gas turbine facility, and in biogas, for example in landfill gas, there are large amount of CO<sub>2</sub> so CO<sub>2</sub> is important diluent too. Dilution method is varying

depending on the dilution placement. There are various dilution placement as fuel-side, air-side, and direct dilution etc. in this study, fuel-side and air-side dilution were examined. Figure 2.6 shows the two dilution placements.

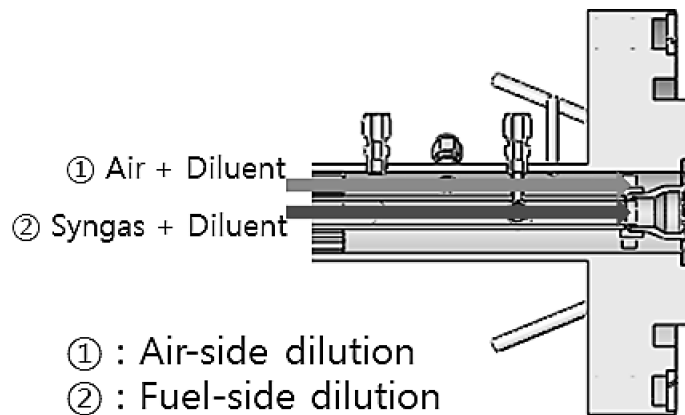


Figure 2.6 Schematic of the dilution placements of the combustor

## **Chapter 3 RESULTS AND DISCUSSION**

### **3.1 NO<sub>x</sub> emission characteristics**

NO<sub>x</sub> emission characteristics of partially premixed syngas flame was investigated and it was based on fuel-side N<sub>2</sub> dilution case. As shown in figure 3.1, NO<sub>x</sub> emission increased as inlet air temperature increased and in figure 3.2, NO<sub>x</sub> emission rose as equivalence ratio rose. Inlet air temperature and equivalence ratio influence flame temperature. When inlet air temperature is low, more heat is lost so flame temperature decreases. For equivalence ratio, flame temperature is related on heat input. We tested with same air flow so increased equivalence ratio meant augmented heat input and flame temperature. Also, in both figure, dilution reduced NO<sub>x</sub> emission because diluent operated as heat sink and it made flame temperature decrease. From these results, we confirmed that thermal NO<sub>x</sub> produced by Zeldovich mechanism in which temperature strongly affects NO<sub>x</sub> formation [1] was dominant in this partially premixed syngas flame.

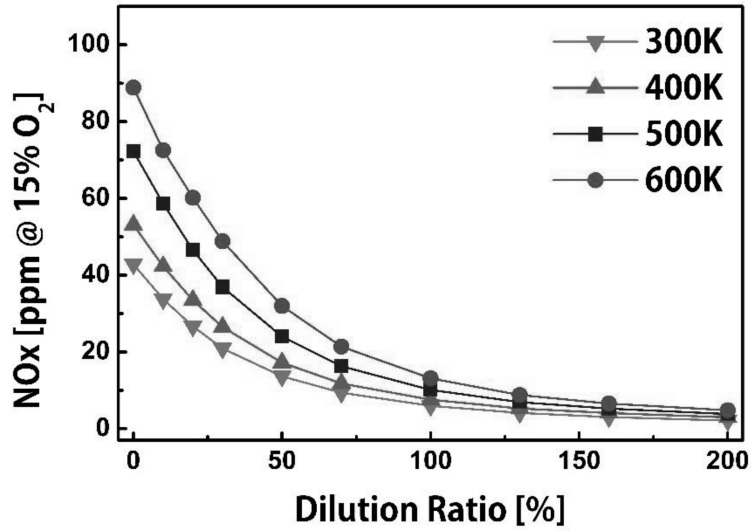


Figure 3.1 NOx concentrations with respect to inlet air temperature.

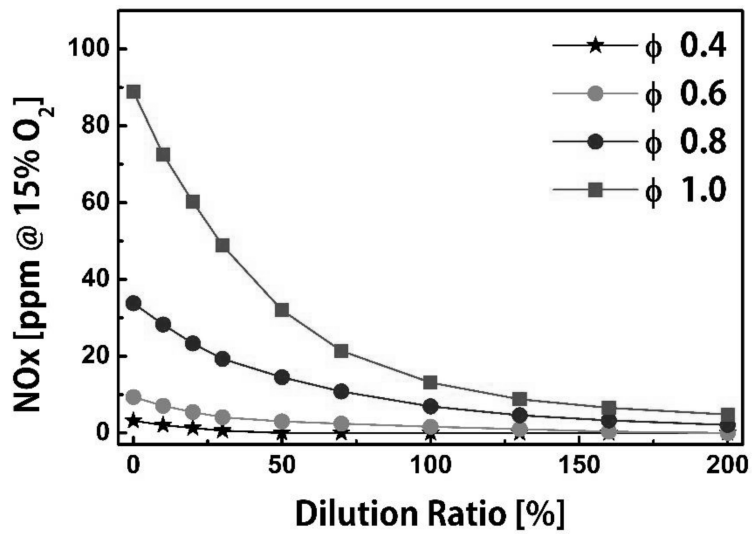


Figure 3.2 NOx concentrations with respect to equivalence ratio,  $T_{inlet}=600K$ .

### 3.1.1 Comparison of diluents

For finding factors that affects NOx emission characteristics of partially premixed H<sub>2</sub>/CO syngas flame, we conducted fuel-side N<sub>2</sub> and CO<sub>2</sub> dilution test. We figured NOx as a function of diluent heat capacity. Diluent heat capacity is defined as following equation.

$$\text{Diluent heat capacity} = \dot{m}_{\text{diluent}} \cdot C_{p,\text{diluent}} \quad (3.1)$$

$\dot{m}_{\text{diluent}}$  is mass flow rate of diluent and  $C_{p,\text{diluent}}$  is specific heat at constant pressure of diluent. Diluent heat capacity is proportional to flame temperature decrease caused by dilution, hence diluent heat capacity is a factor which affects NOx emission characteristics. Also Lee et al. shown that NOx reduction caused by dilution is function of diluent heat capacity [5]. But as shown in figure 3.3 and figure 3.4, at same diluent heat capacity, less NOx was emitted with CO<sub>2</sub> dilution than that with N<sub>2</sub> dilution. From this result, we assumed that there could be other factor to NOx emission characteristics. And we found that the difference between NOx emission with N<sub>2</sub> dilution and that with CO<sub>2</sub> dilution was bigger at high (=1.0) equivalence ratio compared to the difference at low (=0.6) equivalence ratio. We analyzed flame structure to find the factor and a reason for the different difference along equivalence ratio.

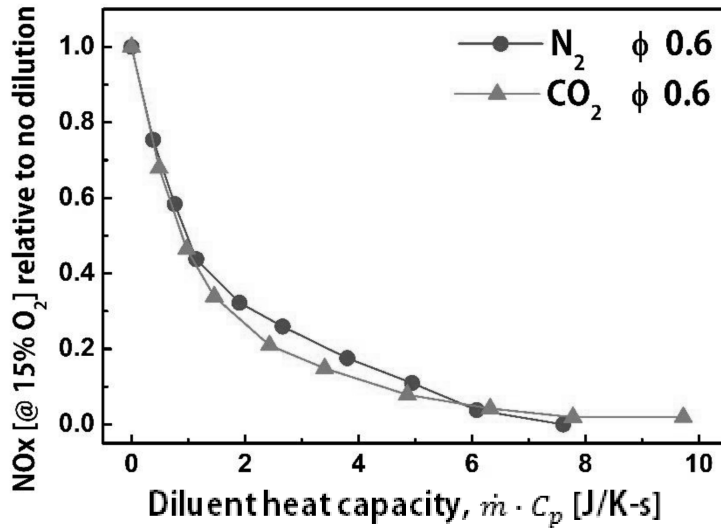


Figure 3.3 NOx concentrations with respect to diluent heat capacity,  $\phi=0.6$ ,  $T_{inlet}=600K$ .

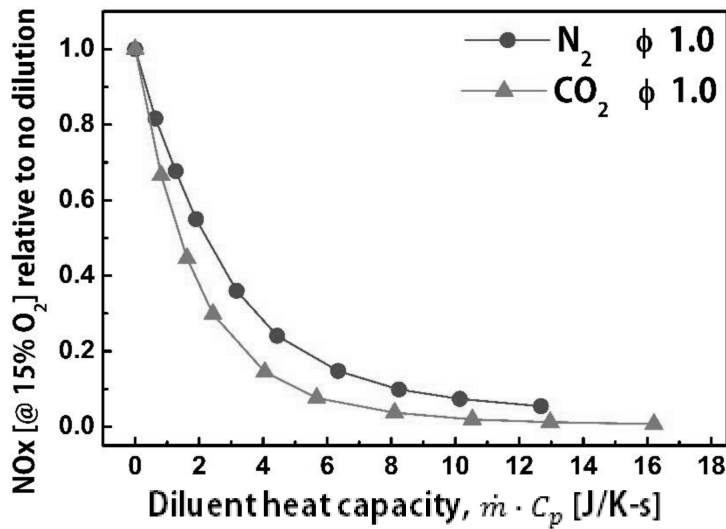


Figure 3.4 NOx concentrations with respect to diluent heat capacity,  $\phi=1.0$ ,  $T_{inlet}=600K$ .



Figure 3.5 is flame image of this combustor and figure 3.6 shows flame structure change as jet momentum ratio increases. Expression of jet momentum ratio is shown in equation (3.2)

$$\text{Jet momentum ratio} = \frac{\text{fuel jet momentum}}{\text{air jet momentum}} = \frac{MW_{\text{fuel}}U_{\text{fuel}}}{MW_{\text{air}}U_{\text{air}}} \quad (3.2)$$

$MW$  is molecular weight and  $U$  is jet velocity. As mentioned in the nozzle description, injected fuel crosses air stream. So, they have similar flow characteristics with jet in crossflow. In jet in crossflow, when jet momentum ratio increases, also penetration and mixing increase. Jet momentum ratio increases as fuel stream flow rate rises and it can be achieved through addition of fuel or diluent flow rate. So, as shown in figure 3.6, when dilution ratio increased, jet momentum ratio also rose and fuel penetration length increased. As a result, flame moved outward. From this result, we could infer that dilution augmented mixedness of fuel and air and it could affect  $\text{NO}_x$  formation. To confirm this, we analyzed  $\text{NO}_x$ , jet momentum ratio and flame images.

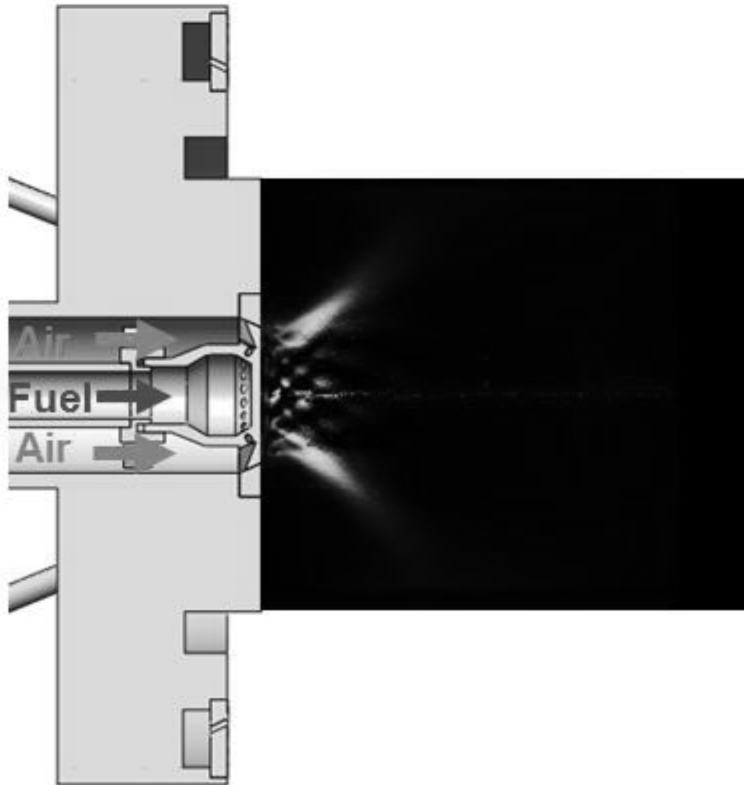
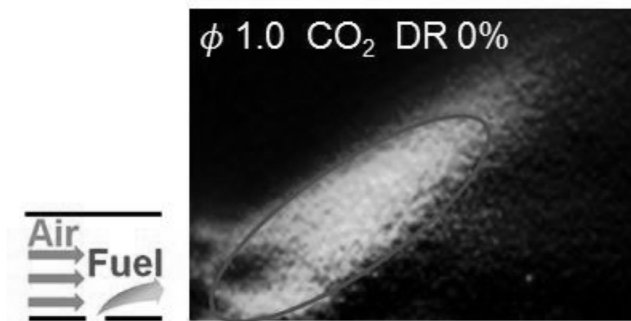


Figure 3.5 Flame image of the combustor.

- **Low jet momentum ratio**



- **High jet momentum ratio**

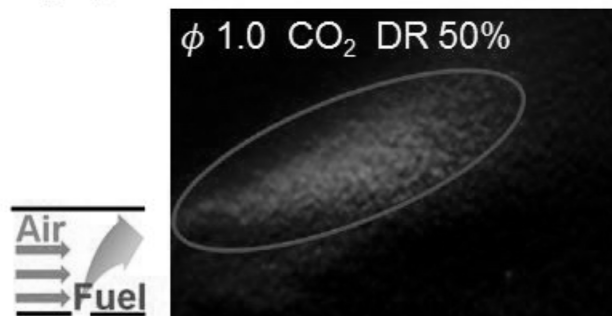


Figure 3.6 Flame structure change depending on jet momentum ratio,  $T_{inlet}=600K$ .

Figure 3.8 shows jet momentum ratio-diluent heat capacity graph. Jet momentum ratio for CO<sub>2</sub> dilution is bigger than that for N<sub>2</sub> dilution because molecular weight of CO<sub>2</sub> is 44 and that of N<sub>2</sub> is 28. To see figure 3.7 and 3.8, there are two circled points. This two points are CO<sub>2</sub> dilution ratio 50%, N<sub>2</sub> dilution ratio 100% at equivalence ratio 1.0 separately. In these points, although diluent heat capacity values are different, NO<sub>x</sub> emission and jet momentum ratio have similar values and it can be seen in flame structure. Table 3.1 shows flame images including these two points. To see images of these two points, they have similar flame structure. From this result, we confirmed that another factor that affected NO<sub>x</sub> emission characteristics was degree of mixing and it is determined by jet momentum ratio. To compare N<sub>2</sub> and CO<sub>2</sub> dilution, jet momentum ratio of CO<sub>2</sub> is bigger than that of N<sub>2</sub> at same diluent heat capacity, so mixedness is bigger with CO<sub>2</sub> dilution and NO<sub>x</sub> formation is less with CO<sub>2</sub> dilution also.

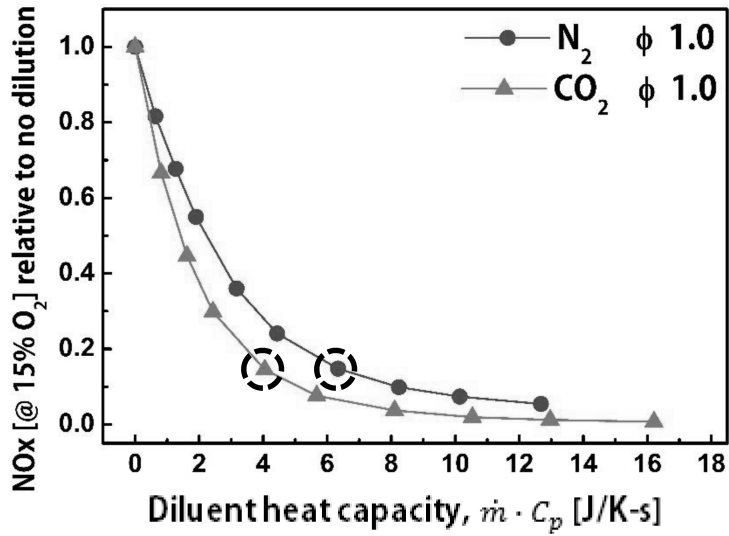


Figure 3.7 NOx concentrations with respect to diluent heat capacity,  $\phi=1.0$ ,  
 $T_{inlet}=600K$ .

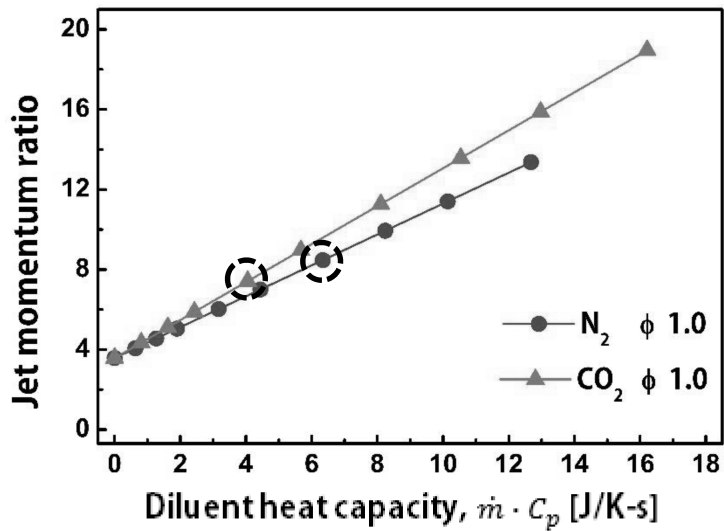


Figure 3.8 Jet momentum ratio with respect to diluent heat capacity,  $\phi=1.0$ .

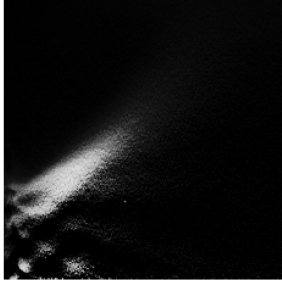
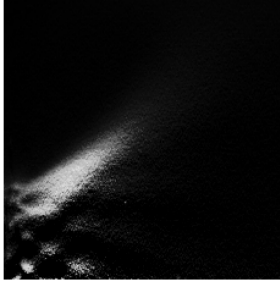
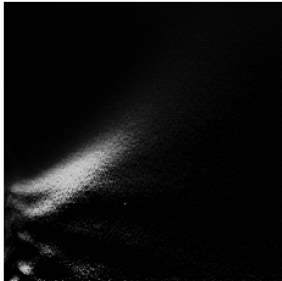
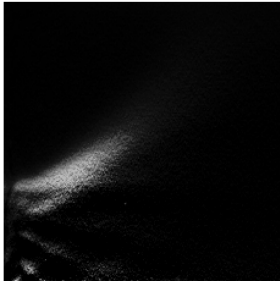
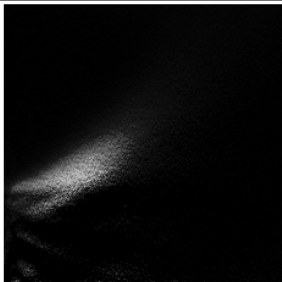
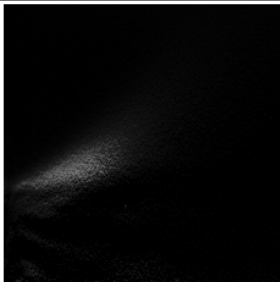
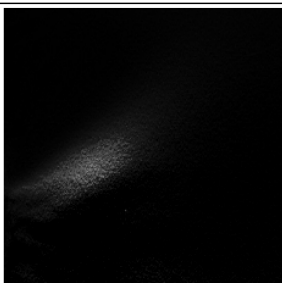
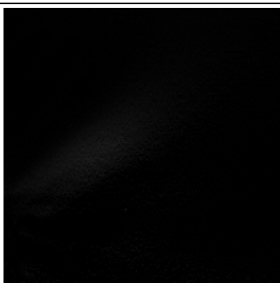
Dilution ratio	$\phi$ 1.0	
	N <sub>2</sub> dilution	CO <sub>2</sub> dilution
0 %		
20 %		
50 %		
100 %		

Table 3.1 Flame structure change depending on dilution ratio (jet momentum ratio) ,  $T_{inlet}=600K$ .

We found another factor but there was still one more question why the difference between  $N_2$  and  $CO_2$  dilution was bigger at high equivalence ratio than that at low equivalence ratio. It is matter of mixedness and figure 3.9 accounts for this. Figure 3.9 shows flame structure map that indicates a boundary line for flame structure change. We fixed a boundary through flame image analysis. When jet momentum ratio was small, flame anchoring point was inside of nozzle. As jet momentum ratio increased, another flame root was formed, and when jet momentum ratio reached value of 4.8, inside root broke and we fixed it as the boundary. The boundary jet momentum ratio value was regular over all equivalence range but boundary diluent heat capacity decreased as equivalence ratio increased due to augmented fuel flow rate. And figure 3.10 and figure 3.11 show the boundary indicated in  $NO_x$  graph. To see  $NO_x$  emission characteristics with dilution, at first  $NO_x$  is reduced sharply by dilution, but after some degree of dilution the slope become small. To compare two equivalence ratio, the boundary line is positioned in sudden drop region at equivalence ratio 1.0, but it is located after that region at equivalence ratio 0.6. So, mixing effect is bigger in the former.

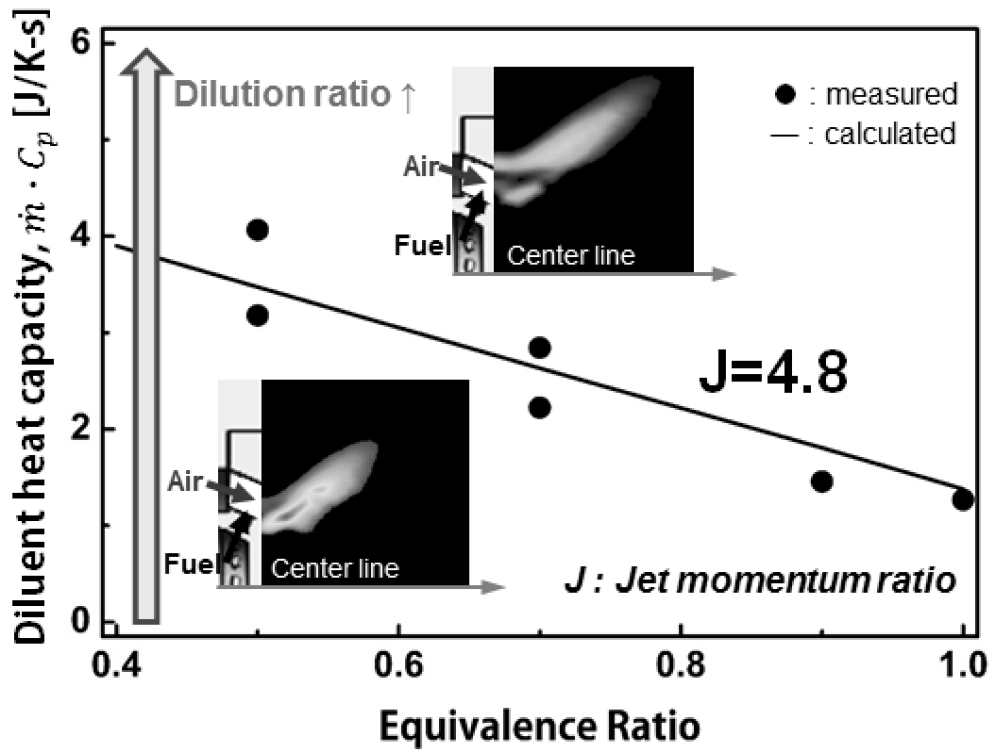


Figure 3.9 Flame structure map,  $T_{inlet}=600K$ .



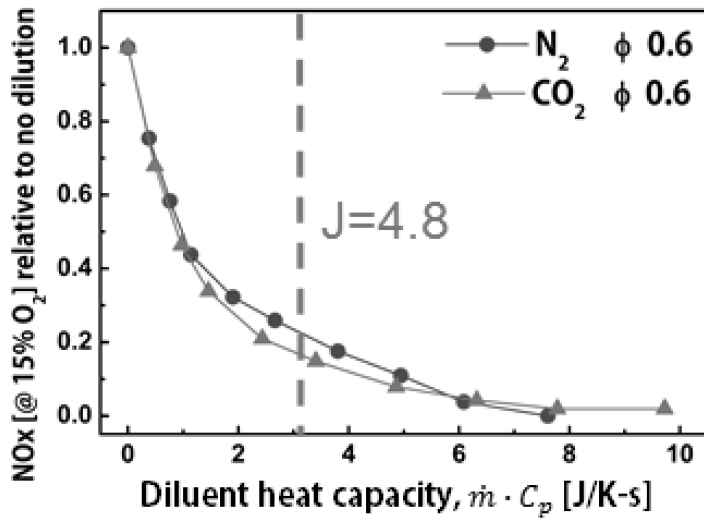


Figure 3.10 NOx concentrations with respect to diluent heat capacity,  $\phi=0.6$ ,  
 $T_{\text{inlet}}=600\text{K}$ .

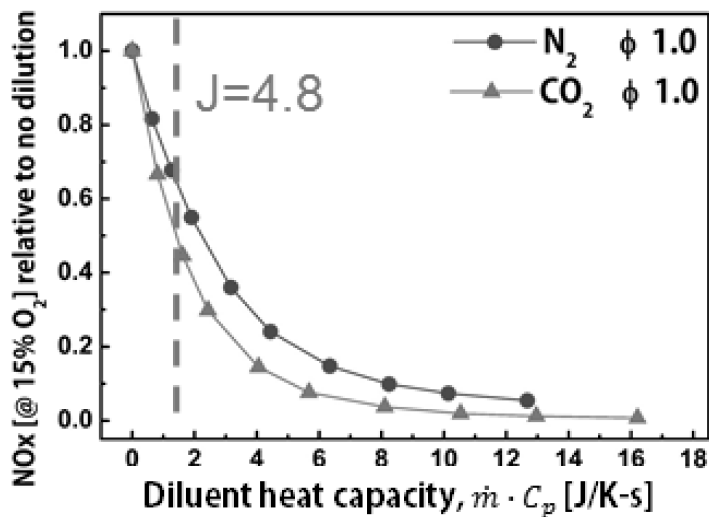


Figure 3.11 NOx concentrations with respect to diluent heat capacity,  $\phi=1.0$ ,  
 $T_{\text{inlet}}=600\text{K}$ .

### 3.1.2 Comparison of dilution placement

It is known that NO<sub>x</sub> emission characteristics changes for different dilution placement. To confirm effect of dilution placement in this combustor, we conducted fuel-side and air-side N<sub>2</sub> dilution test separately. As a result, we gained NO<sub>x</sub>-dilution ratio graph as figure 3.12 and figure 3.13.

NO<sub>x</sub> emission was lower in fuel-side dilution than that in air-side dilution. But, as equivalence ratio increased, the gap became small and when equivalence ratio reached 1.0, they have same value of NO<sub>x</sub> emission. The reason why NO<sub>x</sub> emission in fuel-side dilution was low is that in fuel-stream dilution all diluent passes through flame, but, in air-stream dilution some part of diluent do especially at low equivalence ratio because it is non-premixed combustor and air participate in reaction partly. For this reason effect of flame temperature reduction by dilution is bigger in fuel-side dilution. But, at equivalence ratio become 1, all air react with fuel so all diluent contact the flame front, so the difference between two dilution placement disappears. Weiland and Strakey shown this as peak flame temperature [6]. As mentioned above, this explanation can be verified through figure 3.12 and figure 3.13. In addition, values of NO<sub>x</sub> emission were similar between fuel-side 50% dilution and air-side 100% dilution at equivalence ratio 0.5. It shows that effect of fuel-side dilution is twice as large as that of air-side dilution and this offers another evidence of the explanation.

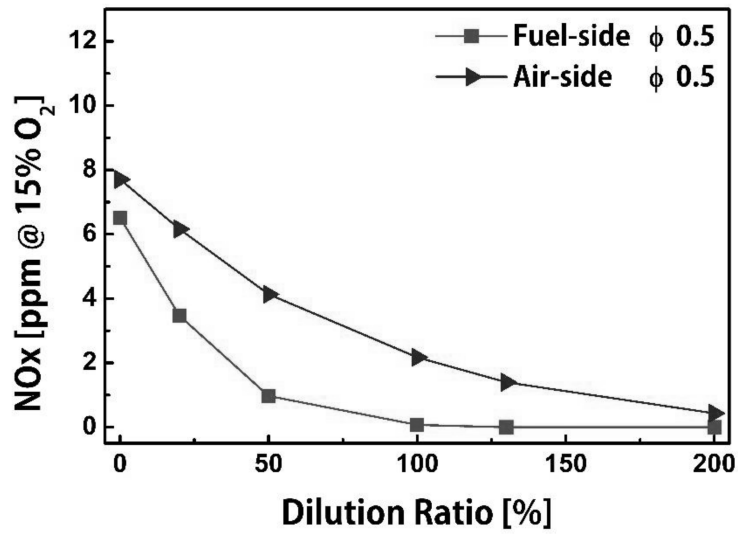


Figure 3.12 NOx concentrations with respect to dilution placement,  $\phi=0.5$ ,  
 $T_{inlet}=600K$ .

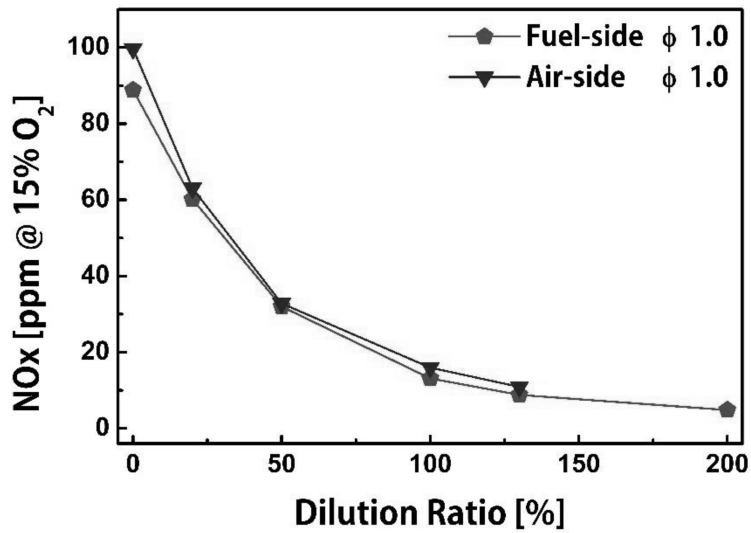


Figure 3.13 NOx concentrations with respect to dilution placement,  $\phi=1.0$ ,  
 $T_{inlet}=600K$ .

We found the other proof in flame image shown in table 3.2. As mentioned before, these images are OH-chemiluminescence image, so high intensity means many OH radicals. In flame, OH radical is formed in reaction region so we can relate it to temperature. Therefore high intensity in image means high temperature. As shown in table 3.2, OH intensity in fuel-side dilution case was less than that in air-side dilution case at equivalence ratio 0.4, but there was little difference at equivalence ratio 1.0. In this combustor, NO<sub>x</sub> consists of thermal NO<sub>x</sub> so these images support the explanation.

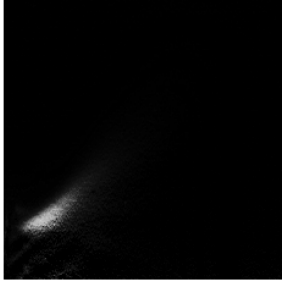

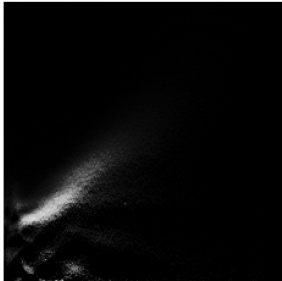
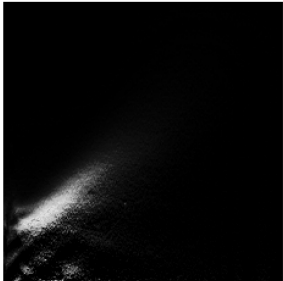
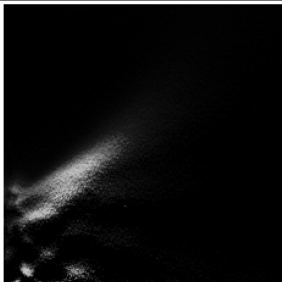
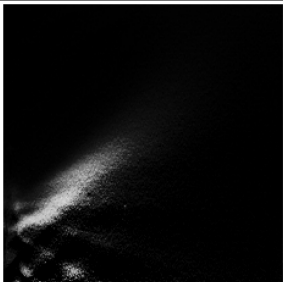
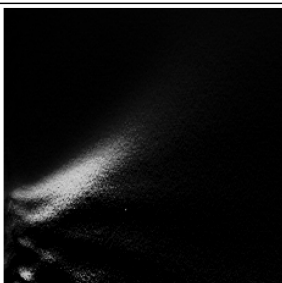
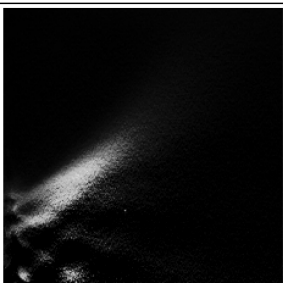
equivalence ratio	Dilution ratio 20 %	
	Fuel-side dilution	Air-side dilution
0.4		
0.6		
0.8		
1.0		

Table 3.2 Flame intensity change depending on dilution placement and dilution ratio,  $T_{inlet}=600K$ .

## 3.2 CO emission characteristics

We studied CO emission characteristics of partially premixed H<sub>2</sub>/CO syngas flame in fuel-side N<sub>2</sub> dilution. As shown in figure 3.14 and figure 3.15, CO emission was below 10 ppm over almost the whole region except equivalence ratio 0.4. CO emission increased sharply as dilution ratio rose and the slope increased as inlet air temperature decreased. In this combustor CO emission seems to be caused by unburned CO because CO emitted largely at lean and cold condition in which CO is combusted incompletely.

Result of comparing N<sub>2</sub> dilution and CO<sub>2</sub> dilution is presented in figure 3.16. CO emitted largely with CO<sub>2</sub> dilution over all region. It is because heat capacity of CO<sub>2</sub> is larger than that of N<sub>2</sub>, so flame temperature with CO<sub>2</sub> dilution is lower than that with N<sub>2</sub> dilution. And this phenomenon was found in comparing dilution placement. As mentioned in 3.1.2, flame temperature was lower in fuel-side dilution and figure 3.17 shows that CO emission in fuel-side dilution is larger than that in air-side dilution. In addition, we conducted diluent pre-heat test and the temperature was set to 600K. As a result CO emission decreased largely because CO was combusted well in this condition. Therefore we concluded that to avoid high CO emission, combustor have to be operated in well combustible region.

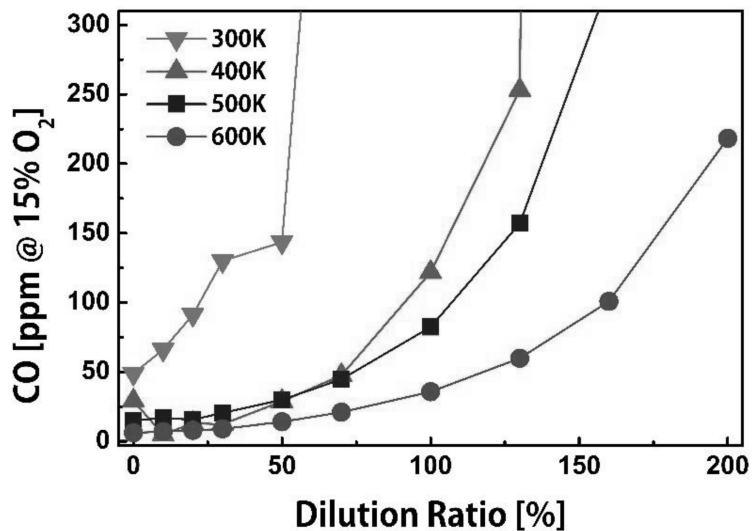


Figure 3.14 CO concentrations with respect to inlet air temperature.

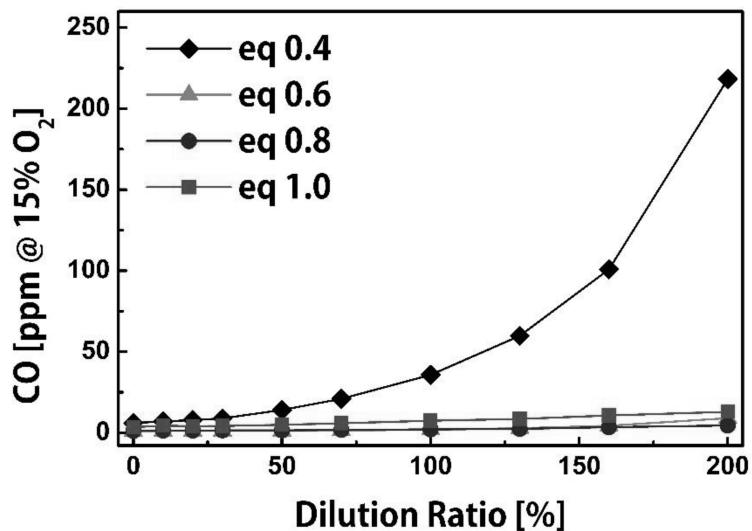


Figure 3.15 CO concentrations with respect to equivalence ratio,  $T_{inlet}=600K$ .

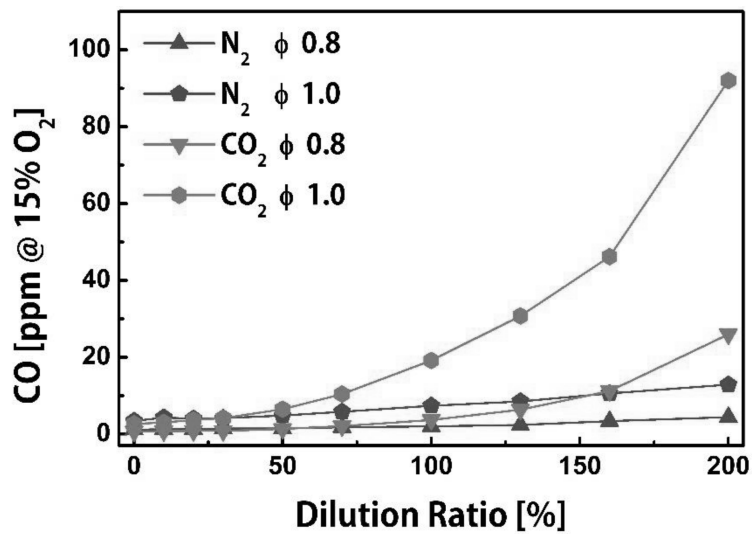
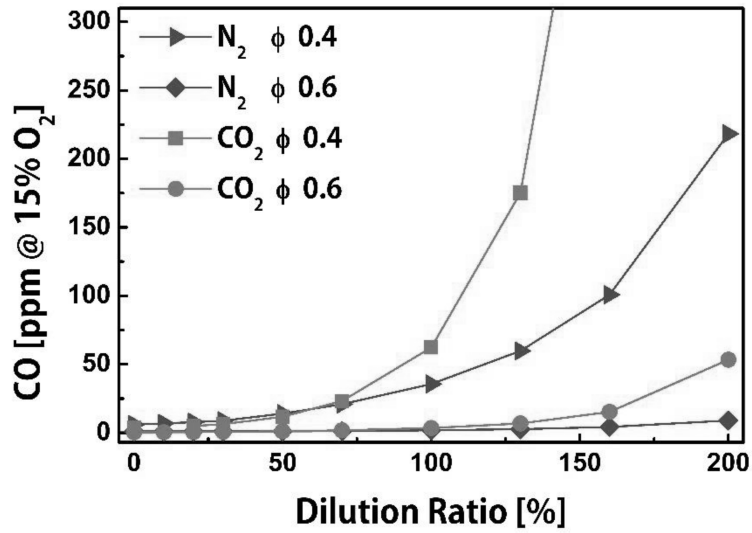


Figure 3.16 CO concentrations with respect to diluent  
 (a) for lean and (b) rich condition,  $T_{inlet}=600K$ .



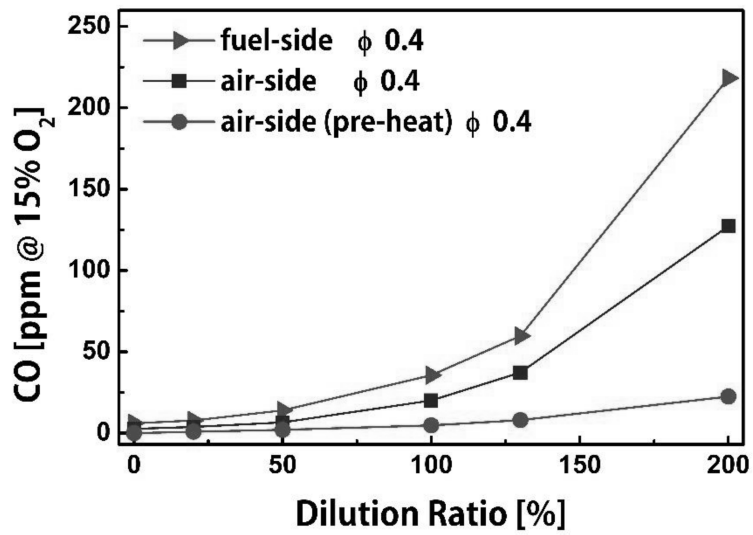


Figure 3.17 CO concentrations with respect to dilution placement,  $T_{inlet}=600K$ .

## Chapter 4 CONCLUSION

We studied emission characteristics of partially premixed H<sub>2</sub>/CO syngas flame in model gas turbine combustor. Especially, we investigated factors which affected emission characteristics. For this objective, we performed experiments varying diluent (N<sub>2</sub> and CO<sub>2</sub>) and dilution placement (fuel-side and air-side), Emission measurement data and OH chemiluminescence image were used to analyze the results.

In this combustor, NO<sub>x</sub> consisted of Thermal NO<sub>x</sub> mainly. So decrease of flame temperature caused by dilution was major factor which affects NO<sub>x</sub> emission characteristics. In addition, by comparing N<sub>2</sub> dilution and CO<sub>2</sub> dilution, we confirmed that mixedness determined by fuel-to-air jet momentum ratio was another factor and it worked above some value of jet momentum ratio. It is because, in the nozzle, injected fuel and air stream intersected like jet-in-crossflow.

Dilution placement was related to dilution efficiency. In fuel-side dilution all diluents passed through flame front but not in air-side dilution because in lean condition some part of oxidizer contacted and reacted with fuel. For this reason, decrease of flame temperature by dilution was bigger in fuel-side dilution and so did NO<sub>x</sub> reduction.

CO was emitted largely when CO of fuel is hard to be combusted. Low equivalence ratio, low temperature due to dilution and low inlet air/diluent temperature made CO hard to be burned.

From these investigation, we suggest two applications. First, in nozzle design, consideration for appropriate jet momentum ratio will produce additional NO<sub>x</sub>

reduction by dilution in partially premixed combustor. Second, to maximize dilution efficiency, low equivalence ratio will be good for operation region except the condition in which unburned CO is emitted largely.

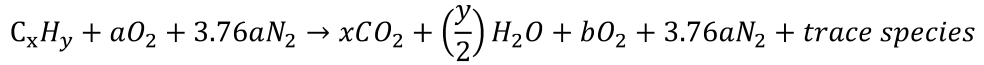
## Appendix A. Correction of Emission Concentration

### A.1 Derivation of equation 2.3

The definition of the correction formula is

$$C_{i, O_2\text{-level } 2} = C_{i, O_2\text{-level } 1} \cdot \frac{N_{mix, O_2\text{-level } 1}}{N_{mix, O_2\text{-level } 2}} \quad - (1)$$

The general reaction of hydrocarbon is



The total mole number of products is calculated as below.

$$a = x + \frac{y}{4} + b$$

$$C_{O_2, dry} = \frac{b}{x + b + 3.76a}$$

$$a = \frac{x + (1 - C_{O_2, dry})y/4}{1 - 4.76C_{O_2, dry}}$$

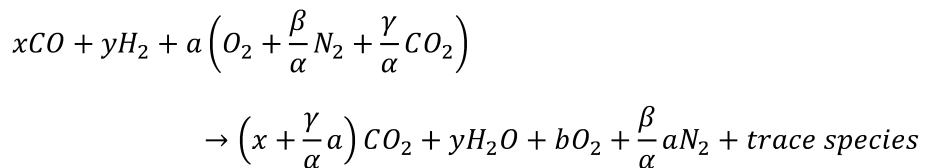
$$N_{mix, dry} = 4.76 \left[ \frac{x + \frac{(1 - C_{O_2, dry})y}{4}}{1 - 4.76C_{O_2, dry}} \right] - \frac{y}{4} = \frac{x + \frac{(1 - C_{O_2, dry})y}{4}}{0.21 - C_{O_2, dry}} - \frac{y}{4} \quad - (2)$$

Substitute (2) for (1)

$$\begin{aligned}
 C_{@ 15\% O_2} &= C_{measured} \left[ \frac{x + \frac{(1 - C_{O_2, dry})y}{4}}{0.21 - C_{O_2, dry}} - \frac{y}{4} \right] \\
 &= C_{measured} \left[ \frac{x + \frac{(1 - 0.15)y}{4}}{0.21 - 0.15} - \frac{y}{4} \right] \\
 &= C_{measured} \left[ \frac{x + \frac{0.79y}{4}}{0.21 - X_{O_2, dry}} \right] \\
 &= C_{measured} \left[ \frac{x + \frac{0.79y}{4}}{0.21 - 0.15} \right] \\
 &= C_{measured} \left( \frac{0.21 - 0.15}{0.21 - X_{O_2, dry}} \right) \\
 &= C_{measured} \left( \frac{21 - 15}{21 - O_{2, measured}} \right)
 \end{aligned}$$

## A.2 Derivation of equation 2.4

The combustion reaction of H<sub>2</sub>/CO syngas with diluents is



The total mole number of the products is

$$N_{mix} = \frac{\left(\frac{1 + C_{O_2, dry}}{2}\right)x + \left(\frac{1 - C_{O_2, dry}}{2}\right)y}{\alpha - C_{O_2, dry}}$$

Therefore, the correction equation is

$$C_{@ 15\% O_2} = C_{measured} \left[ \frac{\left(\frac{1 + C_{O_2, dry}}{2}\right)x + \left(\frac{1 - C_{O_2, dry}}{2}\right)y}{\alpha - C_{O_2, dry}} + \frac{x}{2} - \frac{y}{2} \right] \left[ \frac{\left(\frac{1 + 0.15}{2}\right)x + \left(\frac{1 - 0.15}{2}\right)y}{0.21 - C_{O_2, dry}} + \frac{x}{2} - \frac{y}{2} \right]$$

Because x=71 and y=29 in this study

$$C_{@ 15\% O_2} = C_{measured} \left[ 0.02278 \cdot \frac{\alpha + 2.381}{\alpha - C_{O_2, dry}} \right]$$

## Bibliography

- [1] Stephen R. Turns, “An introduction to combustion concepts and applications-3<sup>rd</sup> edition”, McGraw-Hill international edition, USA, 2012
- [2] S. H. Smith and M. G. Mungal, “Mixing, Structure and Scaling of the Jet in Crossflow”, J. Fluid Mech., 1998
- [3] Kexin Liu and Victoria Sanderson, “The Influence of Changes in Fuel Calorific Value to Combustion Performance for Siemens SGT-300 Dry Low Emission Combustion System”, Fuel, 2013
- [4] K. Boyd Fackler, Megan F. Karalus, Igor V. Novosselov, John C. Kramlich, Philip C. Malte, “Experiential and Numerical Study of NO<sub>x</sub> Formation From the Lean Premixed Combustion of CH<sub>4</sub> Mixed With CO<sub>2</sub> and N<sub>2</sub>”, Journal of Engineering for Gas Turbines and Power, 2011
- [5] Min Chul Lee, Seok Bin Seo, Jisu Yoon, Minki Kim, Youngbin Yoon, “Experimental Study on the Effect of N<sub>2</sub>, CO<sub>2</sub>, and Steam Dilution on the Combustion Performance of H<sub>2</sub> and CO Synthetic Gas in an Industrial Gas Turbine”, Fuel, 2012
- [6] Nathan T. Weiland and Peter A. Strakey, “NO<sub>x</sub> Reduction by Air-Side Versus Fuel-Side Dilution in Hydrogen Diffusion Flame Combustors”, Journal of Engineering for Gas Turbines and Power, 2010
- [7] Chou T. and Oatterson D. J., “In-cylinder Measurement of Mixture Mal-distribution in a L-head Engine”, Combustion and Flame, 1995
- [8] Ahmed M. Elkady, Andrei Evulet, Anthony Brand, Tord Peter Ursin, Arne

- Lynghjem, “Application of Exhaust Gas Recirculation in a DLN F-Class Combustion System for Postcombustion Carbon Capture”, Journal of Engineering for Gas Turbines and Power, 2009
- [9] Milan Kalal and Keith A. Nugent, “Abel Inversion Using Fast Fourier Transforms”, APPLIED OPTICS, 1988
- [10] Lefebvre A. H., Perez R., “Fuel Effects on Gas Turbine Combustion-liner Temperature Pattern Factor and Pollutant Emissions”, Journal of Aircraft, 1984
- [11] Ouimette P., Seers P., “NO<sub>x</sub> Emission Characteristics of Partially Premixed Laminar Flames of H<sub>2</sub>/CO/CO<sub>2</sub> Mixtures”, International Journal of Hydrogen Energy, 2009
- [12] P.M.Anacleto, E.C. Fernandes, S.I.Shtork, "Swirl flow structure and flame characteristics in a model lean premixed combustor", Combust. Sci. and Tech., 2003
- [13] Ying Huang, Vigor Yang, "Dynamics and stability of lean-premixed swirl-stabilized combustion", Progress in Energy and Combustion science, 2009
- [14] F. H. Champagne, S. Kromat, "Experiments on the formation of a recirculation zone in swirling coaxial jets", Experiments in Fluids, 2000
- [15] Kim M., Choi Y., Oh J., Yoon Y., “Flame Vortex Interaction and Mixing Behaviors of Turbulent Non Premixed Jet Flames under Acoustic Forcing”, Combustion and Flame, 2009
- [16] Oh J, Hwang J., Yoon Y., “EINO<sub>x</sub> Scaling in a Non-premixed Turbulent Hydrogen Jet with Swirled Coaxial Air”, International Journal of Hydrogen Energy, 2010
- [17] Laviolette M. and Strawson M., “On the Prediction of Pollutant Emission Indices from Gas Turbine Combustor Chambers”, Proceeding of ASME Turbo Expo,



2008

- [18] Sjoblom B.G. and Odger J., "Factors Limiting Inlet Temperatures", In 5th International Symposium on Airbreathing Engines, 1981
- [19] Mongia, H., and Dodds, W., "Low Emissions Propulsion Engine Combustor Technology Evolution Past, Present and Future," 24<sup>th</sup> Congress of the International Council of the Aeronautical Sciences, 2004
- [20] Doppelheuer, A., and Lecht, M., "Influence of Engine Performance on Emission Characteristics," Symposium on Gas Turbine Engine Combustion, Emissions and Alternative Fuels, 1998
- [21] James J. Feese and Stephen R. Turns, "Nitric Oxide Emissions from Laminar Diffusion Flames: Effects of Air-Side versus Fuel-Side Diluent Addition", Combustion and Flame, 1998
- [22] Kevin J. Whitty, Hongzhi R. Zhang, Eric G. Eddings, "Emissions from Syngas Combustion", Combust. Sci. and Tech., 2008
- [23] Kexin Liu, John P. Wood, Eoghan R. Buchanan, Pete Martin, Victoria E. Sanderson, "Biodiesel as an Alternative Fuel in Siemens Dry Low Emissions Combustors: Atmospheric and High Pressure Rig Testing", Journal of Engineering for Gas Turbines and Power, 2010
- [24] Edmund E. Callaghan and Robert S. Ruggeri, "Investigation of the Penetration of an Air Jet Directed Perpendicularly to an Air Stream", NACA, 1948
- [25] Yasuhiro Kamotani and Isaac Greber, "Experiments on a Turbulent Jet in a Cross Flow", AIAA Journal, 1972
- [26] R. M. Kelso, T. T. Lim, A. E. Perry, "An Experimental Study of Round Jets in Cross-flow", J. Fluid Mech., 1996

- [27] Liying Zhuo, Yong Jiang, Rong Qiu, Jiangtao, An, Wu Xu, “Effects of Fuel-Side N<sub>2</sub>, CO<sub>2</sub>, H<sub>2</sub>O Dilution on Combustion Characteristics and NO<sub>x</sub> Formation of Syngas Turbulent Nonpremixed Jet Flames”, Journal of Engineering for Gas Turbines and Power, 2014
- [28] Arindam Samanta, Ranjan Ganguly, Amitava Datta, “Effect of CO<sub>2</sub> Dilution on Flame Structure and Soot and NO Formations in CH<sub>4</sub>-Air Nonpremixed Flames”, Journal of Engineering for Gas Turbines and Power, 2010
- [29] W. Qin, F. N. Egolfopoulos, T. T. Tsotsis, “Fundamental and Environmental Aspects of Landfill Gas Utilization for Power Generation”, Chemical Engineering Journal, 2001

## 초 록

석탄화력발전은 석탄의 매장량이 풍부하고 값이 싸다는 장점이 있지만 공해물질을 많이 배출한다는 문제점을 갖는다. 석탄가스화 복합발전은 석탄의 가스화 후 탈황, 집진, 그리고 탄소 포집을 통하여 공해문제를 개선한 발전방식으로 전세계적으로 개발 및 건설 중이며 국내에서도 태안에 발전소를 건설 중에 있다. 가스화된 연료에는  $H_2$ 가 많이 포함되어 있기 때문에 역화현상을 방지하기 위하여 비예혼합 연소를 해야 한다. 본 연구에서는 비예혼합 연소 시 발생하는  $NO_x$ 를 제어하기 위한 방법인 희석에 대한 연구를 수행하였다.

희석 시 배출물 특성에 영향을 미치는 요인을 파악하기 위해 GE7EA 노즐을 1/3로 축소 모사한 부분예혼합 타입 모형 가스터빈 연소기에서 희석제와 희석 위치를 바꾸며 연소실험을 수행하였다. 연소기 후단 배기관에서 배출물 농도를 측정하였고, 화염의 OH 자발광을 촬영한 뒤 아벨변환을 통해 화염 단면 이미지를 얻었다.

희석제로  $N_2$ 와  $CO_2$ 를 비교한 결과 희석제에 의한 온도 감소 외에도 다른 요인이  $NO_x$  배출 특성에 영향을 미침을 확인하였고, 화염구조 분석을 통해 연료-공기 분사운동량비에 따른 혼합 정도가  $NO_x$  배출 특성에 영향을 미치는 또 다른 요인임을 확인하였다. 희석위치 변화 실험 결과 공기 희석 시  $NO_x$ 가 더 많이 발생하였고, 이는 희석 위치에 따라 반응영역을 지나는 희석제의 비율이 달라 희석으로 인한 화염온도 저감효과가 달라지기 때문임을 확인하였다. CO는 대부분의 실험 영역에서 10 ppm 이하로 배출되었지만 불완전연소가 일어나는 저당량비 희석 조건에서는 배출량이 급증하는 모습을 보였고, 여러

변수들을 통하여 여기에는 온도가 큰 요인으로 작용함을 확인하였다.

**주요어:** 석탄가스화 복합발전, 가스터빈, NO<sub>x</sub>, 희석제, 희석위치, 화염구조, 분사운동량비

**학 번:** 2013-22485

